

Dynamics of Coupling Functions in Globally Coupled Maps: Size, Periodicity and Stability of Clusters

M. G. Cosenza* and A. Parravano

*Centro de Astrofísica Teórica, Facultad de Ciencias, Universidad de Los Andes,
Apartado Postal 26 La Hechicera, Mérida 5251, Venezuela.*

[Accepted in Phys. Rev. E (2001)]

It is shown how different globally coupled map systems can be analyzed under a common framework by focusing on the dynamics of their respective global coupling functions. We investigate how the functional form of the coupling determines the formation of clusters in a globally coupled map system and the resulting periodicity of the global interaction. The allowed distributions of elements among periodic clusters is also found to depend on the functional form of the coupling. Through the analogy between globally coupled maps and a single driven map, the clustering behavior of the former systems can be characterized. By using this analogy, the dynamics of periodic clusters in systems displaying a constant global coupling are predicted; and for a particular family of coupling functions, it is shown that the stability condition of these clustered states can straightforwardly be derived.

PACS Number(s): 05.45.+b, 02.50.-r

**mcosenza@ciens.ula.ve*

I. INTRODUCTION

There has been much interest in the study of the collective dynamics of chaotic systems subjected to global interactions. Such systems arise naturally in the description of arrays of Josephson junctions, charge density waves, multimode lasers, neural dynamics, evolutionary, chemical and social networks [1–5]. The globally coupled map (GCM) lattice [6] constitutes a prototype model for such global-coupling dynamics. It has recently been argued that GCM systems yield universal classes of collective phenomena [7]. Specifically, a GCM system can exhibit a variety of collective behaviors such as clustering (i.e., the formation of differentiated subsets of synchronized elements in the network) [8]; non-statistical properties in the fluctuations of the mean field of the ensemble [8]; global quasiperiodic motion [9,10]; and different collective phases depending on the parameters of the system [9]. It has been shown that a GCM system is closely related to a single map subjected to an external drive and that this analogy may be used to describe the emergence of clusters in GCM systems in geometrical terms [11].

In particular, the phenomenon of clustering is relevant as it can provide a simple mechanism for segregation, ordering and onset of differentiation of elements in many physical and biological systems. In addition to GCM systems, dynamical clustering has also been found in a globally coupled Rössler oscillators [12], neural networks [13], and coupled biochemical reactions [14]. The interest in this phenomenon has recently grown, since dynamical clusters have been observed experimentally in an array of electrochemical oscillators interacting through a global coupling [15].

In this paper, we investigate the process of cluster formation in general globally coupled map systems by focusing on the dynamics of their global coupling functions. In most studies on GCM systems, the mean field of the network has been used as the global coupling function. Here, we study GCM systems subjected to different global coupling functions and show how they can be analyzed under a common framework. We investigate how the distribution of elements among a few clusters and their periodicities depend on the functional form of the global coupling.

Section II contains a description of the dynamics of different global coupling functions in GCM systems and a calculation of the possible periodicities and cluster sizes when two clusters emerge in these systems. The driven map analogy is employed in Sec. III to interpret the clustering behavior of GCM systems. In Sec. IV the dynamical properties of periodic clusters in systems exhibiting a constant global coupling are predicted; and for a particular family of global coupling functions, the stability condition for these clustered states is derived in an Appendix. Conclusions are presented in Sec. V.

II. DYNAMICS OF GLOBAL COUPLING FUNCTIONS

Consider a general globally coupled map system

$$x_{t+1}(i) = (1 - \epsilon)f(x_t(i)) + \epsilon H(x_t(1), x_t(2), \dots, x_t(N)), \quad (1)$$

where $x_t(i)$ gives the state of the element i ($i = 1, 2, \dots, N$) at discrete time t ; N is the size of the system; ϵ is the coupling parameter; $f(x)$ describes the (nonlinear) local dynamics, which in the present article is chosen to be the quadratic map $f(x) = 1 - rx^2$; and $H_t(x_t(1), x_t(2), \dots, x_t(N))$ is the global coupling function. We shall consider a general class of global coupling functions of N variables such that $H(\dots, x_t(i), \dots, x_t(j), \dots) = H(\dots, x_t(j), \dots, x_t(i), \dots)$, $\forall i, j$; that is, H is assumed to be invariant to argument permutations. This property of the coupling function ensures that, at any time, each element of the globally coupled system is subjected to the same influence of the coupling term. Some examples of coupling functions belonging to this class are

$$H = \langle x \rangle = \frac{1}{N} \sum_{i=1}^N x_t(i); \quad (2)$$

$$H = \langle f \rangle = \frac{1}{N} \sum_{i=1}^N f(x_t(i)); \quad (3)$$

$$H = \Delta x = \sqrt{\frac{1}{N} \sum_{i=1}^N (x_t(i) - \langle x \rangle)^2}; \quad (4)$$

$$H = \bar{x} = \prod_{i=1}^N |x_t(i)|^{\frac{1}{N}}. \quad (5)$$

The first two examples correspond to forward and backward mean field coupling, respectively, and they have been widely used in GCM studies. The third global coupling function is the usual dispersion or mean square deviation of N variables, and it may describe systems whose elements do not interact when they are synchronized. This kind of global interaction might be relevant in some biological or social systems where the members of a community are driven by their deviations from the mean behavior. The last example is the geometric mean. This type of multiplicative coupling occurs, for instance, in a system of N sequential amplifiers where the gain of element i is a function of the magnitude of its state $x_t(i)$, and H is proportional to the total gain of the system. Many statistical functions of N variables share the property of invariance under argument permutations and they could as well be taken as global coupling functions in GCM systems given by Eq.(1).

For some range of its parameters the GCM system in Eq.(1) reaches an asymptotic collective behavior characterized by the segregation of the elements into K clusters, each exhibiting a period P , where the k th cluster has a number N_k of elements, with $\sum_{k=1}^K N_k = N$. The fraction p_k of elements in the k th cluster is $p_k = N_k/N$. The evolution of the k th cluster may be described by a variable $\chi_t(k)$ which gives the common state of the N_k elements belonging to this cluster at time t . The periodic orbit adopted by the state $\chi_t(k)$ of the k th cluster can be expressed as a sequence of P values $[\chi_1(k), \chi_2(k), \dots, \chi_P(k)]$. The specific partition $\{p_1, p_2, \dots, p_K\}$ into K clusters and the specific values taken by the periodic orbit of each cluster depend on initial conditions and parameters of the system.

When a GCM system falls into K periodic clusters, the coupling function H also shows a periodic motion. As an illustration of this behavior, Fig. 1(a) shows a typical situation in which a GCM system, with global coupling function $H = \bar{x}$, displays two clusters, each in period two. In this case, the coupling function follows a period-two motion.

Collective states consisting of two clusters have recently been observed in an experimental array of globally interacting chemical elements [15]. This clustered collective state is interesting to analyze in globally coupled maps. In this simple situation, there is a fraction p of elements in one cluster and a fraction $(1 - p)$ in the other cluster. Thus the global coupling functions from Eqs.(2)-(5) simplify to:

$$H = \langle x \rangle = p\chi_t(1) + (1 - p)\chi_t(2), \quad (6)$$

$$H = \langle f \rangle = pf(\chi_t(2)) + (1 - p)f(\chi_t(1)), \quad (7)$$

$$H = \Delta x = \sqrt{p(1 - p)(\chi_t(2) - \chi_t(1))^2}, \quad (8)$$

$$H = \bar{x} = |\chi_t(1)|^p |\chi_t(2)|^{(1-p)}. \quad (9)$$

When the GCM system reaches a two-cluster state, the dynamics of the system reduces to the two coupled maps

$$\chi_{t+1}(1) = (1 - \epsilon)f(\chi_t(1)) + \epsilon H, \quad (10)$$

$$\chi_{t+1}(2) = (1 - \epsilon)f(\chi_t(2)) + \epsilon H; \quad (11)$$

where $H = H(\chi_t(1), \chi_t(2), p)$ is the reduced, two-cluster coupling function, as in Eqs.(6)-(9). If both cluster states $\chi_t(1)$ and $\chi_t(2)$ fall in period-two orbits, the coupling function H follows, in general, a period-two motion, as shown

in Fig. 1(a), although H may become constant in some circumstances (see Fig. 1(b) and Sec. IV). Let H_1 and H_2 be the values adopted alternatively in time by H in its period-two orbit for a given partition $\{p, 1-p\}$, as indicated on Fig. 1(a). The values H_1 and H_2 depend on i) the functional form of H ; ii) the parameters of the GCM system Eq.(1); and iii) the fraction p .

Consider then several GCM systems with the same parameters $r = 1.7$ and $\epsilon = 0.2$ but with different coupling functions such as those in Eqs. (2)-(5). Two clusters in period two can emerge in each of these systems for some range of the fraction p . The resulting asymptotic orbits $[H_1, H_2]$ of the respective coupling functions are shown in Fig. 2(a) as p varies, giving rise to a curve in each case. Note that each function H possesses period-two orbits only for a limited range of the fraction p . Figure 2(b) is a magnification of Fig. 2(a) which shows that the dynamics of the backward and the mean field coupling functions become equal for $p = 0.5$; i.e., when the two clusters have equal sizes. In this case, both coupling functions reach the constant value $H_1 = H_2 = 0.365$. Notice that the dispersion coupling function, $H = \Delta x$, only displays states with $H_1 = H_2$; that is, even when the two clusters in period two may have different sizes, this particular global coupling always reaches a stationary value. The curves for the other coupling functions are symmetrical with respect to the diagonal in Fig. 2(b), which they cross for $p = 0.5$. On the diagonal, the coupling functions are constant and the two clusters evolve out of phase with respect to each other (Sec. IV).

Note also that the different global coupling functions perform a period-two motion only on a restricted region of the plane (H_1, H_2) . It will be shown in Sec. III that period-two orbits of any permutable coupling function will fall within the dashed contour in Fig. 2.

In general, a coupling function H of a GCM system in a collective state of two clusters can reach various asymptotic periodic orbits for appropriate initial conditions. Each Fig. 3(a) to 3(d) shows the regions on the space of parameters (p, ϵ) for which a coupling function H of a GCM in a two-cluster state displays different periodic motions. The local parameter is fixed at $r = 2$. Figures 3(a) and 3(b) correspond to the backward and forward mean field coupling, respectively. Note the very different distributions of periodic regions for the coupling functions in Figs. 3(a) and 3(b). It should be noticed that, besides the collective periodic states for two clusters shown in Figs. 3(a)-3(d), there can exist other states in a GCM system consisting of more than two periodic clusters for the same values of the parameters r and ϵ , but corresponding to different initial conditions.

The inverse problem of determining the global coupling function in experimental systems is relevant since in general the specific functional form of the acting coupling is not known. This can be a complicated problem because, in addition, the exact form of the local dynamics may not be extracted in most situations. However, if the local dynamics is known some insight on the function H of a globally coupled system can be gained within the framework presented here. For example, in the case of a dynamical system showing two period-two clusters with partition p , the resulting asymptotic orbit $[H_1, H_2]$ can be obtained by measuring the cluster orbits and using Eqs. (10) and (11). For different realizations of partition p , the curve $[H_1, H_2]$ can be drawn as a function of p on the plane (H_1, H_2) , and compared with curves $[H_1, H_2]$ corresponding to known functional forms H such as those in Fig. 2.

III. DRIVEN MAP ANALOGY

As shown in Ref. [11], the clustering behavior of GCM systems can be analyzed through its analogy with the dynamics of a single map subjected to an external drive. In order to interpret the results of the preceding section, let us consider an associated driven map

$$s_{t+1} = (1 - \epsilon)f(s_t) + \epsilon L_t, \quad (12)$$

where s_t is the state of the map at discrete time t , $f(s_t)$ is the same local dynamics as in Eq.(1), and L_t is an external driving term assumed to be periodic with period P . We denote the sequence of P values adopted by the periodic drive L_t by $[L_1, L_2, \dots, L_P]$. The analogy between a GCM system and a driven map arises because in the former system (Eq. (1)) all the elements are affected by the global coupling function in exactly the same way at all times, and therefore the behavior of any element $x_t(i)$ in the GCM is equivalent to the behavior of a single driven map (Eq. (12)) with $L_t = H$ and initial condition $s_o = x_o(i)$. Additionally, if a GCM system reaches a clustered, periodic collective state, its corresponding coupling function H follows in general a periodic motion. Thus the associated driven map (Eq. (12)) with a periodic drive L_t should display a behavior similar to that of an element belonging to a periodic cluster in the GCM system. In particular, periodic drives resulting in periodic orbits of s_t in Eq. (12) may be employed to predict the emergence of clustered, periodic states in a GCM (Eq. (1)), regardless of the specific functional form of the global coupling H and without doing direct simulations on the entire GCM system.

The driven map is multistable; i.e., there can exist several attractors for the same parameter values r and ϵ . Specifically, for a given periodic drive $[L_1, L_2, \dots, L_P]$, the map s_t may reach a number of distinct asymptotic responses $\bar{s}_t(j)$; ($j = 1, 2, \dots, J$), all with the same period, and depending on initial conditions. The orbits of s_t with period M

can be expressed as a sequence of values $[\bar{s}_1(j), \bar{s}_2(j), \dots, \bar{s}_M(j)]$. The correspondence between a GCM system (Eq. (1)) in a state of K clusters with period P and its associated driven map (Eq. (12)) can be established when $M = P$ and $J = K$.

Using this analogy, the main features in Fig. 2 can now be explained. In terms of a driven map subjected to a period-two drive $L_t = [L_1, L_2]$ and the same parameters $r = 1.7$ and $\epsilon = 0.2$ as in the GCM systems considered in Fig. 2, the bounded region on that figure contains the values of L_1 and L_2 for which the driven map s_t just possesses two distinct asymptotic orbits ($J = 2$) of period two ($M = 2$), denoted by $[\bar{s}_1(1), \bar{s}_2(1)]$ and $[\bar{s}_1(2), \bar{s}_2(2)]$. For values of L_1 and L_2 outside this diamond shaped region, the map s_t may also reach a number of asymptotic periodic orbits but none with both $J = 2$ or $M = 2$, at least on the interval $-1 \leq L_1, L_2 \leq 1$. Because of the analogy drawn above, all period-two motions $[H_1, H_2]$ of permutable coupling functions in GCM systems given by Eq. (1) with $r = 1.7, \epsilon = 0.2$ and displaying two clusters in period two will fall on this bounded region of the plane (H_1, H_2) . Equivalently, a collective state of two clusters in period two can emerge in a GCM system only if its global coupling function has an orbit $[H_1, H_2]$ with values $H_1 = L_1$ and $H_2 = L_2$ contained within the bounded region of Fig. 2. The boundaries of that region vary as the parameters r and ϵ are changed. It is out of the scope of the present work to establish how the bounded region for two clusters in period two, as well as other regions for different clustered, periodic states, depend on parameters. However, it is worth noticing that this dependence can serve to characterize GCM systems with permutable coupling functions, and that this characterization can be obtained by the sole use of an associated driven map.

The analogy between a GCM system with a given coupling function H in a two-cluster state and an associated driven map can be carried further by defining an associated coupling function [11]

$$\Theta_H = H(\bar{s}_t(1), \bar{s}_t(2), p); \quad (13)$$

that is, Θ_H is similar to the reduced two-cluster coupling function, such as Eqs.(6)-(9) but with the arguments $\chi_t(1)$ and $\chi_t(2)$ from the cluster trajectories replaced by the driven map orbits $\bar{s}_t(1)$ and $\bar{s}_t(2)$. The associated coupling function links the dynamics of clusters in a GCM system to the dynamics of a single associated driven map. The function Θ_H depends on the functional form of the coupling function H , on the partition $\{p, 1-p\}$ among the two clusters in the GCM, and on the orbits $\bar{s}_t(1)$ and $\bar{s}_t(2)$, which themselves are function of the period-two drive $[L_1, L_2]$ and the parameters r and ϵ . Thus for fixed r and ϵ , and a given H , we have $\Theta_H = \Theta_H(L_1, L_2, p)$. The main point is that, an equivalence between a GCM system Eq. (1) in a two-cluster, period-two state, and an associated driven map, Eq. (12), with a period-two drive occurs when the following conditions are fulfilled

$$\Theta_H(\bar{s}_1(1), \bar{s}_1(2), p) = L_1, \quad (14)$$

$$\Theta_H(\bar{s}_2(1), \bar{s}_2(2), p) = L_2. \quad (15)$$

Eqs. (14)-(15) constitute a set of two nonlinear equations for L_1 and L_2 , for a given p . The solution $[L_1^*, L_2^*]$ of Eqs. (14)-(15) predicts that the GCM possesses a state characterized by the coupling function motion $[H_1 = L_1^*, H_2 = L_2^*]$ and cluster orbits $[\chi_1(1), \chi_2(1)] = [\bar{s}_1(1), \bar{s}_2(1)]$, $[\chi_1(2), \chi_2(2)] = [\bar{s}_1(2), \bar{s}_2(2)]$. The succession of solutions $[L_1^*, L_2^*]$, as p varies, yields the curve corresponding to a given H in Fig. 2. Thus, each curve on the plane (H_1, H_2) is parameterized by the fraction p . Moreover, there exist solutions $[L_1^*, L_2^*]$ to Eqs. (14)-(15) only for an interval of p . Therefore, the curves in Fig. 2 can, in principle, be calculated *a priori* by using an associated driven map and just the specific functional form of H in each case. The range of possible cluster sizes, described by the values of the fraction p for which exist solutions to Eqs. (14)-(15), can also be predicted by this method. Similarly, the regions of period two in Figs. 3(a)-3(d) can be obtained by varying the parameter ϵ and calculating the interval of p for which Eqs. (14)-(15) have solutions.

IV. PREDICTION AND STABILITY OF CLUSTERS IN SYSTEMS WITH CONSTANT GLOBAL COUPLING

Another simple clustered collective state in GCM systems occurs when the coupling function H remains constant in time, i.e., $H = C$. This behavior may take place in a GCM system with a permutable coupling function when K clusters, each having N/K elements and period K , are evolving with shifted phases in order to yield a constant value for H . That is, if the periodic orbits of K identical-size clusters are cyclically permuting in time, the resulting H becomes constant. For those collective states, the behavior of any of such clusters in the GCM system can be emulated by an associated driven map subjected to a constant forcing $L_t = C$ [16]. In the case of a GCM displaying two equal size clusters in period two, this situation corresponds to the intersection of H with the diagonal in Fig. 2. The cluster orbits are then related as $\chi_t(1) = [\chi_1(1), \chi_2(1)] = [a, b]$ and $\chi_t(2) = [\chi_1(2), \chi_2(2)] = [b, a]$. On the other

hand, the associated driven map with $L_t = C$ has a unique asymptotic period-two orbit $\bar{s}_t = [\alpha, \beta]$ on a range of C , where α and β are functions of C . The associated coupling function Θ_H also simplifies in such case. For the reduced, two-cluster couplings in Eqs (6)-(9), the corresponding associated coupling functions become

$$\Theta_{\langle x \rangle}(\alpha, \beta) = \frac{1}{2}(\alpha + \beta) \quad (16)$$

$$\Theta_{\langle f \rangle}(\alpha, \beta) = \frac{1}{2}[f(\alpha) + f(\beta)] \quad (17)$$

$$\Theta_{\Delta x}(\alpha, \beta) = \frac{1}{2}|\alpha - \beta| \quad (18)$$

$$\Theta_{\bar{x}}(\alpha, \beta) = |\alpha|^{1/2}|\beta|^{1/2}. \quad (19)$$

Then Eqs. (14)-(15) with $L_1 = L_2 = C$ reduce to the single equation

$$\Theta_H(\alpha, \beta) = C, \quad (20)$$

which can be seen as an equation for C , for given values of the parameters ϵ and r . The solution $C = C_*$ of Eq. (20) provides a complete description of the GCM state since then $a = \alpha(C_*)$, $b = \beta(C_*)$ and $H = C_*$. Figure 4 shows the bifurcation diagram of s_t , Eq. (12), as a function of the constant drive $L_t = C$ up to period two, with fixed parameters $r = 2$ and $\epsilon = 0.4$. The fixed point region in this diagram corresponds to one stationary cluster (i.e., a synchronized collective state) in the GCM, Eq. (1), with constant H . The period-two window corresponds to the values α and β adopted by the driven map on this range of C . Once $\alpha(C)$ and $\beta(C)$ are known from the bifurcation diagram, the function $\Theta_H(C)$ associated to any global coupling function in a GCM can be readily obtained, assuming that the GCM is in a state of two equal size clusters ($p = 0.5$), evolving out of phase with respect to each other. In Figure 4, the Θ_H functions associated to the four global couplings in Eqs.(2)-(5) with fixed ϵ are shown as function of C . As stated above, the solutions C_* to Eq. (20) correspond to states in GCM systems with a coupling function reaching a stationary value $H = C_*$. Thus, the intersections of the Θ_H curves with the diagonal in Fig. 4 give all the possible states of GCM systems that maintain a constant H , either with one stationary cluster (if the intersection occurs on the fixed point window of the bifurcation diagram of s_t) or with two clusters in period two (if the intersection occurs on the period two window of the diagram). Note that both the backward and the forward mean field couplings have the same two-cluster, period-two solution $\langle x \rangle = \langle f \rangle = C_* = 0.416$, but these couplings have different functional dependence on the constant drive $L_t = C$. The coincidence of the couplings $\langle x \rangle$ and $\langle f \rangle$ for $p = 0.5$ was already seen in Fig. 2(b). Similarly, the geometric mean coupling $H = \bar{x}$ gives only one two-cluster, period-two solution at $\bar{x} = C_* = 0.305$. In contrast, the dispersion global coupling, $H = \Delta x$, has three intersections with the diagonal: one corresponds to the synchronized stationary state in the associated GCM, with $\Delta x = C_* = 0$, and the other two correspond to different clustered states of the GCM, each consisting of two equal size clusters in period two, with $\Delta x = C_* = 0.083$ and $\Delta x = C_* = 0.25$, respectively. All the states predicted by the intersections of the different Θ_H with the diagonal in Fig. 4, except one, are readily found in simulations on the corresponding GCM systems for appropriated initial conditions in each case. Actually, for a GCM with the coupling $H = \Delta x$, the predicted two-cluster, period-two state with $\Delta x = C_* = 0.083$ is unstable: it is never achieved in simulations on the GCM system, even when the initial conditions are chosen very close to that state. What is observed, instead, is the evolution of the GCM system towards either the stationary one cluster state with $\Delta x = 0$ or the two-cluster, period-two state with $\Delta x = 0.25$. Thus, in addition to being predicted by the solutions of the equation $\Theta_H = C$, the observed clustered states of a GCM displaying constant coupling must be stable, which implies some stability condition on the solutions. It can be shown (see Appendix) that for coupling functions satisfying $\sum_{i=1}^N \partial H / \partial x_i = 0$, the condition $d\Theta_H/dC > 1$ at the intersection with the diagonal implies that the corresponding solution is unstable. This is the case of the global coupling $H = \Delta x$. Note that the solution at $C_* = 0.083$ is the only one for which $\frac{d\Theta}{dC}|_{C_*} > 1$ in Fig. 4 and therefore it is unstable, independently of the cluster fraction p . For the coupling $H = \langle f \rangle$, a stability analysis of states consisting of two or three clusters in period three has been performed by Shimada and Kikuchi [17]. However, the simple criterium for instability $\frac{d\Theta}{dC}|_{C_*} > 1$ does not apply for $H = \langle f \rangle$.

Constant coupling functions may also occur in GCM systems with different cluster sizes; that is the case of a GCM possessing dispersion global coupling $H = \Delta x$ and displaying two clusters with any partition $\{p, 1-p\}$, as seen in Fig. 1(b). Figure 5 shows the associated function $\Theta_{\Delta x}$ with fixed ϵ as a function of the constant drive C for several values of the fraction p . There exist a critical fraction $p_c = 0.25$ below which only one solution corresponding to one stationary cluster, i.e., synchronization, can appear in the GCM system. Above this critical fraction, two states, each consisting of two clusters in period two, are additionally predicted by the solutions $C = C_*$ of $\Theta_{\Delta x} = C$. These solutions emerge as a pair: one solution is always unstable since $d\Theta_H/dC|_{C_*} > 1$ there, and the other is the one two-cluster, period-two collective state with constant Δx that is actually observed in simulations on the corresponding GCM system. For the fraction $p_c = 0.25$, there is a two-cluster, period-two solution $\Theta_{\Delta x} = C_* = 0.125$ that is marginally stable.

V. CONCLUSIONS

Most studies on GCM lattices and other globally coupled systems have assumed mean field coupling. However, other forms of global coupling may be relevant in some situations. We have analyzed, in a general framework, the clustering behavior in GCM systems subjected to permutable global coupling functions by considering the dynamics of the coupling functions.

We have shown that different GCM systems can be represented by the orbits of their coupling functions on a common space. For simplicity, only collective states in GCM systems consisting of two clusters in period two were considered. We have shown that the functional form of the global coupling in a GCM system determines the periodicity of its motion and the possible distributions of elements among the clusters. The existence of a well defined interval of possible partitions among two clusters, out of which no clusters emerge in the system, has been observed experimentally [15]. In experimental or natural situations where clustering occurs, the specific functional form of the coupling is in general unknown. The present study may be useful to obtain insight into the acting global coupling function in practical situations.

We have employed a previously introduced analogy between a GCM system and a single externally driven map [11] in order to give a unified interpretation of the observed clustering behavior of the GCM systems considered in this article. A periodically driven map with local periodic windows can display multiple asymptotic periodic responses which are similar to cluster orbits in a GCM system with permutable H . This analogy implies that dynamical clustering can occur in any GCM system with a permutable coupling function and periodic windows in the local dynamics. The presence of windows of stable periodic orbits in the local map is essential for the emergence of clusters. In fact, no clustering is observed in a GCM system if the local maps do not have periodic windows [18]; what is observed instead is synchronization or nontrivial collective behavior, i.e., an ordered temporal evolution of statistical quantities coexisting with local chaos.

The associated coupling function derived from the driven map analogy is particularly simple to use in the prediction of clustered states in GCM systems with two equal size clusters and exhibiting constant global coupling $H = C$. The associated coupling function Θ_H can be directly constructed from the bifurcation diagram of the steadily driven map. The cluster states are obtained from the solutions of Eq. (20) and can be represented graphically in a simple way. Although Eq. (20) has been used for the case of two clusters in period two, it can also be applied to find GCM states consisting of K equal size clusters in period K . In addition, the associated coupling function Θ_H carries information about the stability of the predicted two-cluster states. In particular, for the family of coupling function satisfying property (A9), the stability condition of clustered states in a GCM with constant $H = C_*$ is directly given by the slope $d\Theta_H/dC|_{C_*}$. The example of a GCM system with dispersion coupling function $H = \Delta x$ reveals that a constant coupling can also be maintained by clusters of different sizes. Our method based on Eq. (20) also predicts successfully the cluster states in these situations.

The driven map analogy suggests that the emergence of clusters should be a common phenomenon which can be expected in various dynamical systems formed by globally interacting elements possessing stable periodic orbits on some parameter range of their individual dynamics. The examples presented here show that progress in the understanding of the collective behavior of globally coupled systems can be achieved by investigating their relation to a driven oscillator.

ACKNOWLEDGMENT

This work has been supported by Consejo de Desarrollo Científico, Humanístico y Tecnológico of the Universidad de Los Andes, Mérida, Venezuela.

APPENDIX: ON THE RELATION BETWEEN STABILITY AND THE ASSOCIATED COUPLED FUNCTION

Consider a general GCM system with any global permutable coupling function. Suppose that the system reaches a state consisting of two clusters. Then the dynamics of the system reduces to two coupled maps Eqs. (10)-(11), i.e.,

$$\begin{aligned}\chi_{t+1}(1) &= (1 - \epsilon)f(\chi_t(1)) + \epsilon H(\chi_t(1), \chi_t(2), p) = F(\chi_t(1), \chi_t(2)), \\ \chi_{t+1}(2) &= (1 - \epsilon)f(\chi_t(2)) + \epsilon H(\chi_t(1), \chi_t(2), p) = G(\chi_t(1), \chi_t(2)).\end{aligned}\tag{A1}$$

If the two clusters are in period-two orbits, the stability of this collective state in the GCM is given by the eigenvalues of the product of Jacobian matrices

$$\mathbf{J} = \mathbf{J}_1 \mathbf{J}_2 = \prod_{i=1}^2 \begin{pmatrix} \frac{\partial F}{\partial \chi_i(1)} & \frac{\partial F}{\partial \chi_i(2)} \\ \frac{\partial G}{\partial \chi_i(1)} & \frac{\partial G}{\partial \chi_i(2)} \end{pmatrix}. \quad (\text{A2})$$

If the two clusters move out of phase, the asymptotic state of the GCM can be described by the two orbits $\chi_t(1) \equiv [\chi_1(1), \chi_2(1)] = [a, b]$ and $\chi_t(2) \equiv [\chi_1(2), \chi_2(2)] = [b, a]$, which satisfy

$$\begin{aligned} b &= (1 - \epsilon)f(a) + \epsilon H(a, b, p), \\ a &= (1 - \epsilon)f(b) + \epsilon H(a, b, p). \end{aligned} \quad (\text{A3})$$

For the local dynamics $f(x) = 1 - rx^2$, one gets

$$\mathbf{J}_1 = \begin{pmatrix} -2(1 - \epsilon)ra + \epsilon H_a & \epsilon H_b \\ \epsilon H_a & -2(1 - \epsilon)rb + \epsilon H_b \end{pmatrix}, \quad (\text{A4})$$

$$\mathbf{J}_2 = \begin{pmatrix} -2(1 - \epsilon)rb + \epsilon H_b & \epsilon H_a \\ \epsilon H_b & -2(1 - \epsilon)ra + \epsilon H_a \end{pmatrix}, \quad (\text{A5})$$

where

$$H_a \equiv \left. \frac{\partial H(\chi_t(1), \chi_t(2))}{\partial \chi_t(1)} \right|_{\chi_t(1)=a, \chi_t(2)=b} = \left. \frac{\partial H(\chi_t(1), \chi_t(2))}{\partial \chi_t(2)} \right|_{\chi_t(1)=b, \chi_t(2)=a}, \quad (\text{A6})$$

and

$$H_b \equiv \left. \frac{\partial H(\chi_t(1), \chi_t(2))}{\partial \chi_t(2)} \right|_{\chi_t(1)=a, \chi_t(2)=b} = \left. \frac{\partial H(\chi_t(1), \chi_t(2))}{\partial \chi_t(1)} \right|_{\chi_t(1)=b, \chi_t(2)=a}. \quad (\text{A7})$$

Consider now the dispersion coupling function, Eq. (4). This coupling belongs to the family of functions of N variables

$$H(x_1, x_2, \dots, x_N) = \sum_{i=1}^N h_e(x_i - \langle x \rangle), \quad (\text{A8})$$

where h_e is any even function of its argument. It can be straightforwardly shown that this family of functions possesses the property

$$\sum_{i=1}^N \frac{\partial H}{\partial x_i} = 0. \quad (\text{A9})$$

Therefore, in a two cluster state, any H in this family of global coupling functions satisfies

$$\frac{\partial H(\chi_t(1), \chi_t(2))}{\partial \chi_t(1)} + \frac{\partial H(\chi_t(1), \chi_t(2))}{\partial \chi_t(2)} = 0. \quad (\text{A10})$$

If the two clusters evolve out of phase with respect to each other, and additionally the GCM has a coupling H with property (A9), then the two eigenvalues of the matrix \mathbf{J} in Eq. (A2) become identical and their value is

$$\lambda = 2r\epsilon(\epsilon - 1)(aH_b + bH_a) + 4r^2ab(\epsilon - 1)^2. \quad (\text{A11})$$

The stability criterion of this state is given by the modulus of the eigenvalue λ ; that is, $|\lambda| > 1$ ($|\lambda| < 1$) implies that the state is unstable (stable). The values a and b are, respectively, the values of α and β at the intersection of the function $\Theta_{\Delta x}$ with the diagonal in Fig. 4.

Let us analyze the relationship between the eigenvalue λ and the derivative $d\Theta_{\Delta x}/dC$ at the intersection points with the diagonal in Fig. 4 or Fig. 5. In general,

$$\frac{d\Theta}{dC} = \frac{\partial \Theta}{\partial \alpha} \frac{\partial \alpha}{\partial C} + \frac{\partial \Theta}{\partial \beta} \frac{\partial \beta}{\partial C}, \quad (\text{A12})$$

where

$$\alpha = \frac{-1 + R}{2r(\epsilon - 1)}, \quad (\text{A13})$$

$$\beta = \frac{-1 - R}{2r(\epsilon - 1)}, \quad (\text{A14})$$

and

$$R = (-3 - 4r\epsilon^2 C + 4r\epsilon C + 4r - 8r\epsilon + 4r\epsilon^2)^{1/2}. \quad (\text{A15})$$

Since

$$\frac{\partial \alpha}{\partial C} = -\frac{\partial \beta}{\partial C} = \frac{1}{2r(\epsilon - 1)} \frac{\partial R}{\partial C} = -\frac{\epsilon}{R}, \quad (\text{A16})$$

then

$$\frac{d\Theta}{dC} = -\frac{\epsilon}{R} \left(\frac{\partial \Theta}{\partial \alpha} - \frac{\partial \Theta}{\partial \beta} \right). \quad (\text{A17})$$

Since $\Theta_{\Delta x}$ has the same functional form as $H = \Delta x$, then $\Theta_{\Delta x}$ also satisfies property (A10), that is

$$\frac{\partial \Theta_{\Delta x}}{\partial \alpha} = -\frac{\partial \Theta_{\Delta x}}{\partial \beta}, \quad (\text{A18})$$

and therefore

$$\frac{d\Theta_{\Delta x}}{dC} = -\frac{2\epsilon}{R} \frac{\partial \Theta_{\Delta x}}{\partial \alpha}. \quad (\text{A19})$$

Let $C = C_*$ be a value of C corresponding to the intersection of $\Theta_{\Delta x}$ with the diagonal in Fig. 4. Then $\alpha(C_*) = a$ and $\beta(C_*) = b$; and $\Theta_{\Delta x}(C_*) = H(a, b)$, which gives

$$\left. \frac{d\Theta_{\Delta x}}{dC} \right|_{C_*} = -\frac{2\epsilon}{R} H_a. \quad (\text{A20})$$

Using the fact that $H_a = -H_b$ from Eq. (A10), the eigenvalue λ becomes

$$\lambda = 2r\epsilon(\epsilon - 1)H_a(b - a) + 4r^2 ab(\epsilon - 1). \quad (\text{A21})$$

Eqs.(A13) and (A14) with $C = C_*$ give the values a and b , respectively. Then, substitution of these values and H_a from Eq.(A20) in Eq. (A21) yields

$$\lambda = R^2 \left(\left. \frac{d\Theta_{\Delta x}}{dC} \right|_{C_*} - 1 \right) + 1. \quad (\text{A22})$$

Therefore, the condition $d\Theta/dC|_{C_*} > 1$ implies that $|\lambda| > 1$, and thus the two-cluster, period-two solution with $C_* = 0.07$ given by the intersection of $\Theta_{\Delta x}$ with the diagonal in Fig. 4 is unstable. Similarly, the solutions C_* of $\Theta_{\Delta x} = C$ for the different curves in Fig. 5 for which $d\Theta/dC|_{C_*} > 1$, are unstable.

Note that the above stability result for $H = \Delta x$ is also valid for any global coupling function satisfying property (A9).

[1] P. Hadley and K. Wiesenfeld, *Phys. Rev. Lett.* **62**, 1335 (1989).

[2] K. Wiesenfeld, C. Bracikowski, G. James, and R. Roy, *Phys. Rev. Lett.* **65**, 1749 (1990).

- [3] S. H. Strogatz, C. M. Marcus, R. M. Westervelt, and R. E. Mirollo, *Physica D* **36**, 23 (1989).
- [4] N. Nakagawa and Y. Kuramoto, *Physica D* **75**, 74 (1994).
- [5] K. Kaneko, *Complexity* **3**, 53 (1998).
- [6] K. Kaneko, *Physica D* **41**, 137 (1990).
- [7] K. Kaneko and I. Tsuda, *Complex Systems: Chaos and Beyond* (Springer, Berlin, 2000).
- [8] K. Kaneko, *Physica D* **86**, 158 (1995).
- [9] K. Kaneko, *Physica D* **54**, 5 (1991).
- [10] A. Pikovsky and J. Kurths, *Physica D* **76**, 411 (1994).
- [11] A. Parravano and M. G. Cosenza, *Phys. Rev. E* **58**, 1665 (1998).
- [12] D. H. Zanette and A. S. Mikhailov, *Phys. Rev. E* **57**, 276 (1998).
- [13] D. H. Zanette and A. S. Mikhailov, *Phys. Rev. E* **58**, 872 (1998).
- [14] Ch. Furusawa and K. Kaneko, *Phys. Rev. Lett.* **84**, 6130 (2000).
- [15] W. Wang, I. Z. Kiss, and J. L. Hudson, *Chaos* **10**, 248, (2000).
- [16] A. Parravano and M. G. Cosenza, *Int. J. Bifurcations Chaos* **9**, 2311 (1999).
- [17] T. Shimada and K. Kikuchi, *Phys. Rev. E* **62**, 3489 (2000).
- [18] M. G. Cosenza and J. Gonzalez, *Prog. Theor. Phys.* **100**, 21 (1998).

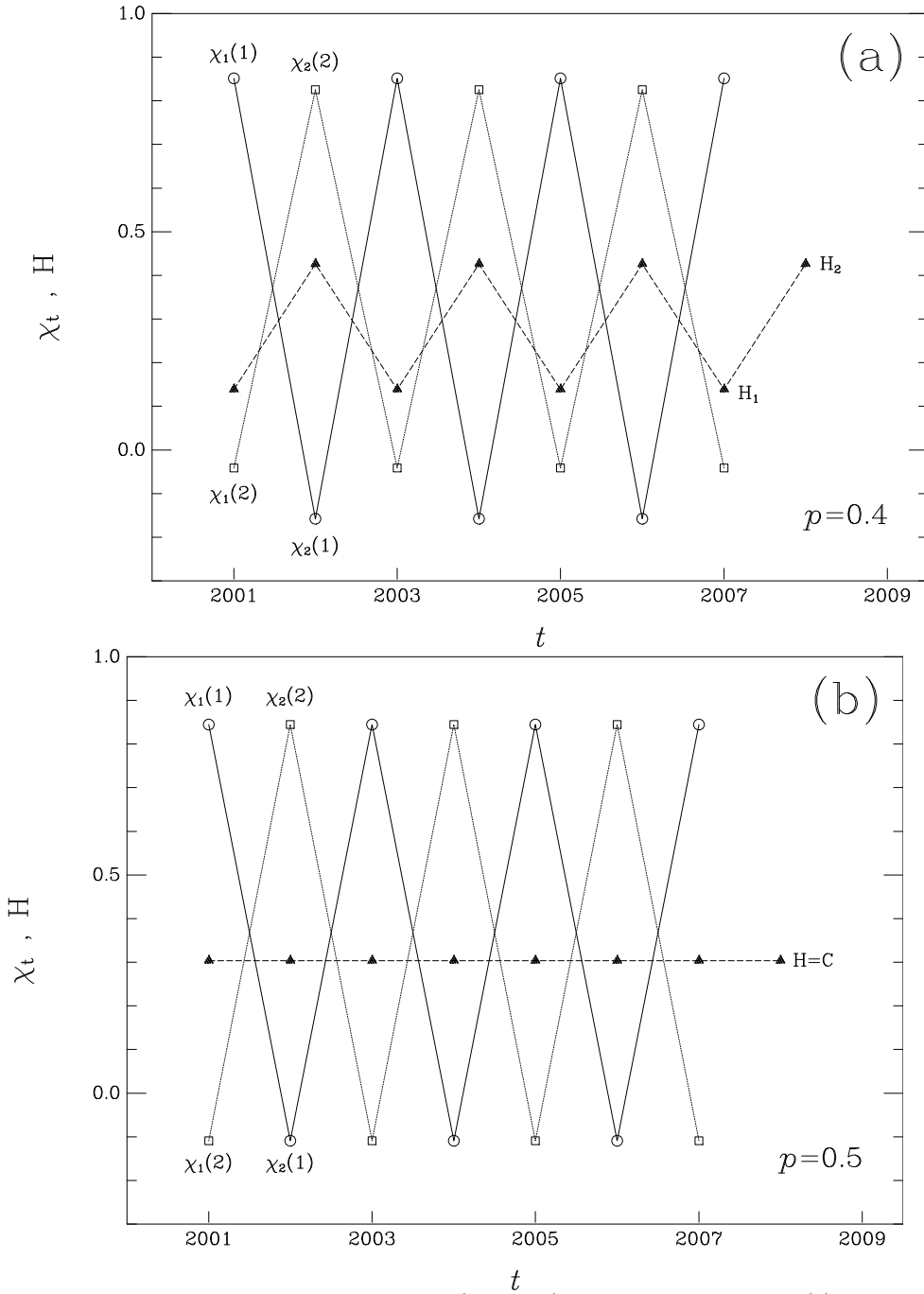


FIG. 1. Dynamics of the coupling $H = \bar{x}$ (triangles) in a GCM system Eq. (1) with parameters $r = 1.7$, $\epsilon = 0.2$, displaying two clusters, each in period two. Cluster orbits are $\chi_t(1) = [\chi_1(1), \chi_2(1)]$ (circles) and $\chi_t(2) = [\chi_1(2), \chi_2(2)]$ (squares). (a) For the partition $p = p_1 = 0.4$ and $p_2 = 0.6$, H follows a period-two motion, adopting the values $[H_1, H_2]$. (b) For ($p = 0.5$), the two clusters evolve out of phase with respect to each other and H remains constant at the value $H = C = 0.3037$.

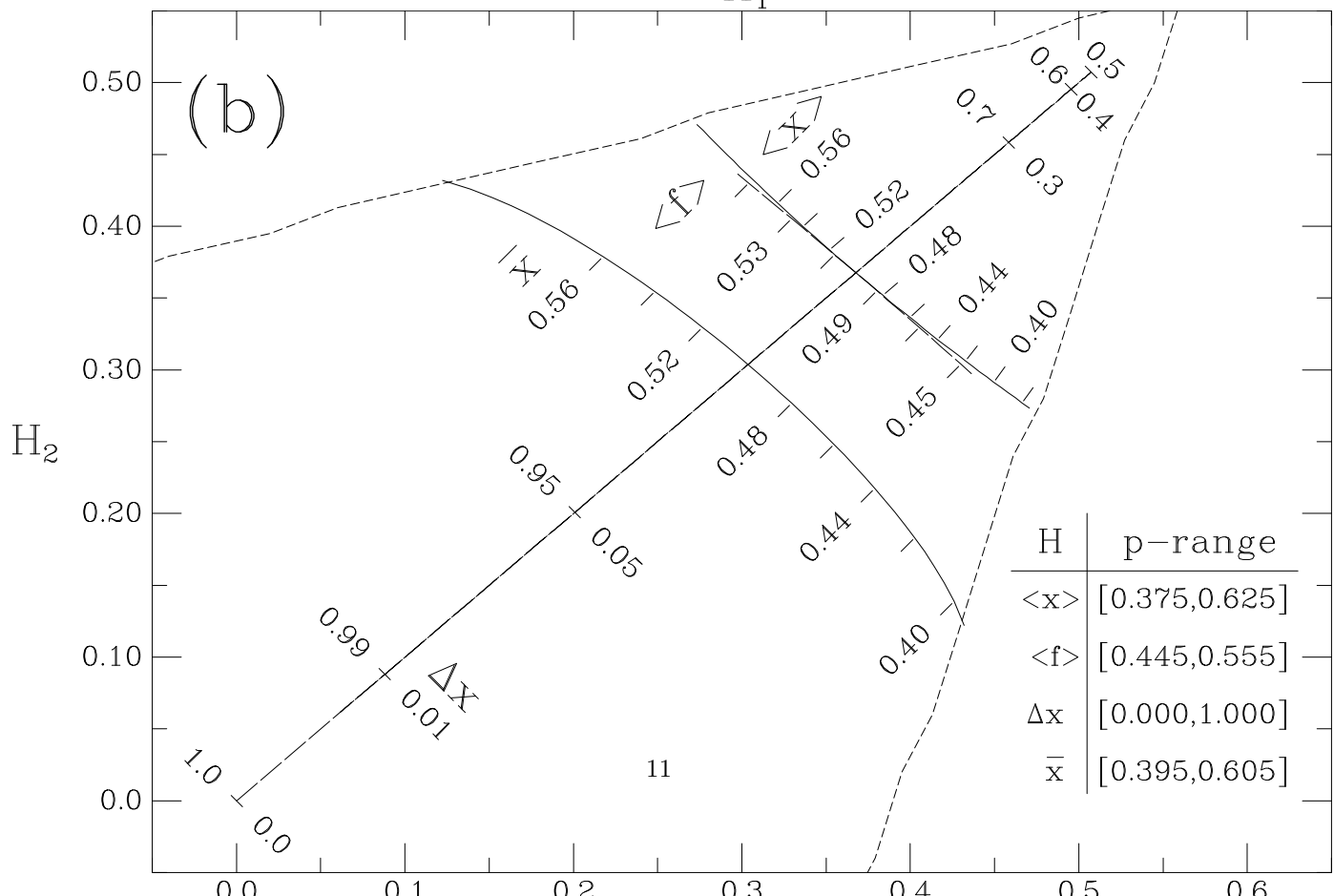
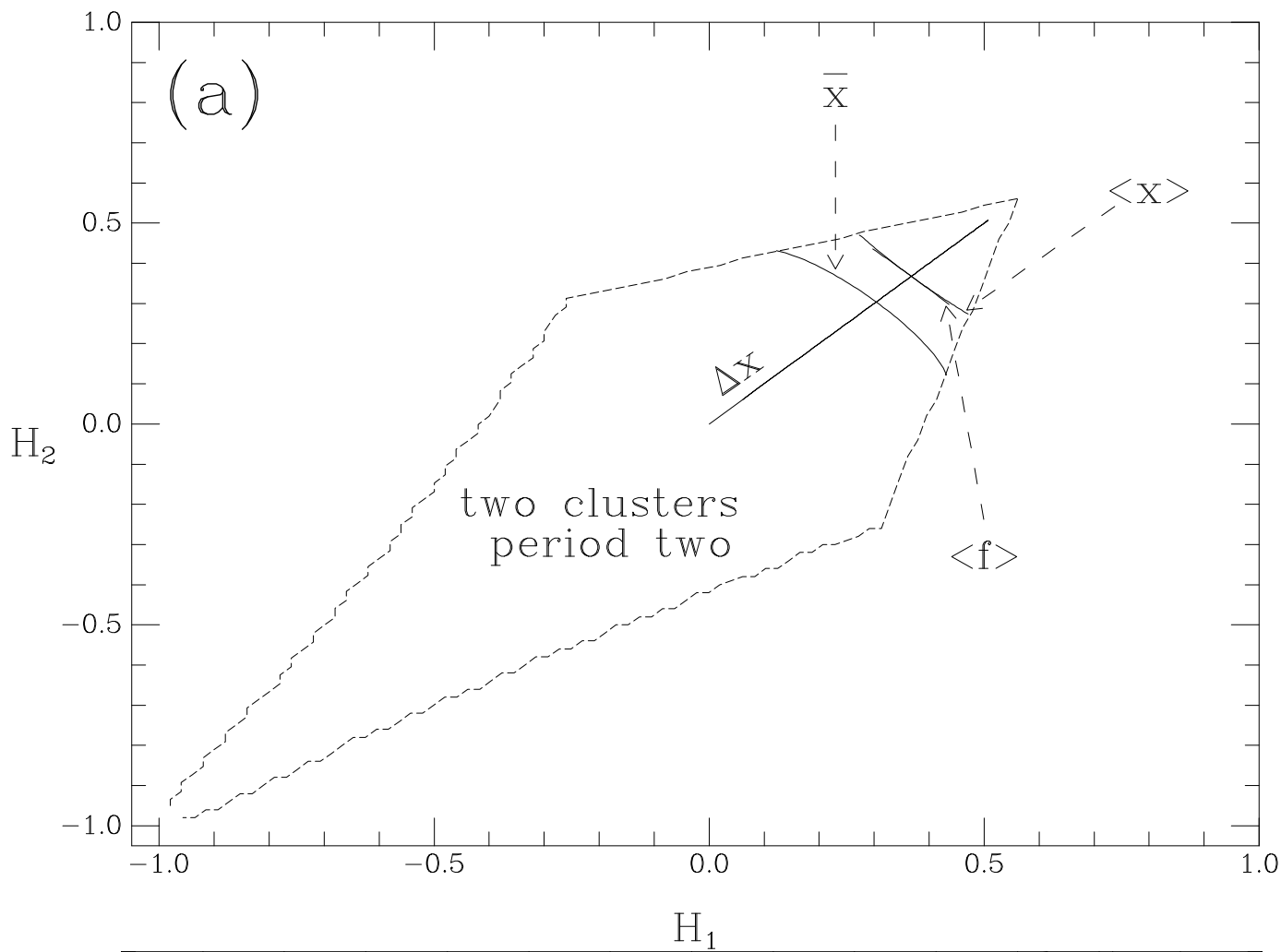


FIG. 2. a) Curves of period-two orbits $[H_1, H_2]$ on the plane (H_1, H_2) as p varies for the four coupling functions Eqs. (6)-(9) in corresponding GCM systems displaying two clusters. Parameters are the same for the four systems, $r = 1.7$, $\epsilon = 0.2$. The boundaries of the region where period-two orbits of any permutable H may take place is indicated with dashed lines. b) Magnification of a). Labels identify the curve associated to each H and the numbers besides the marks along each curve indicate the corresponding values of the cluster fraction p . The range of possible values of p for the different curves is also displayed on the figure.

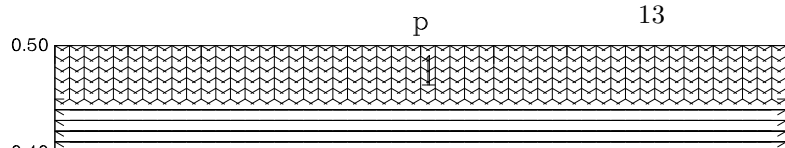
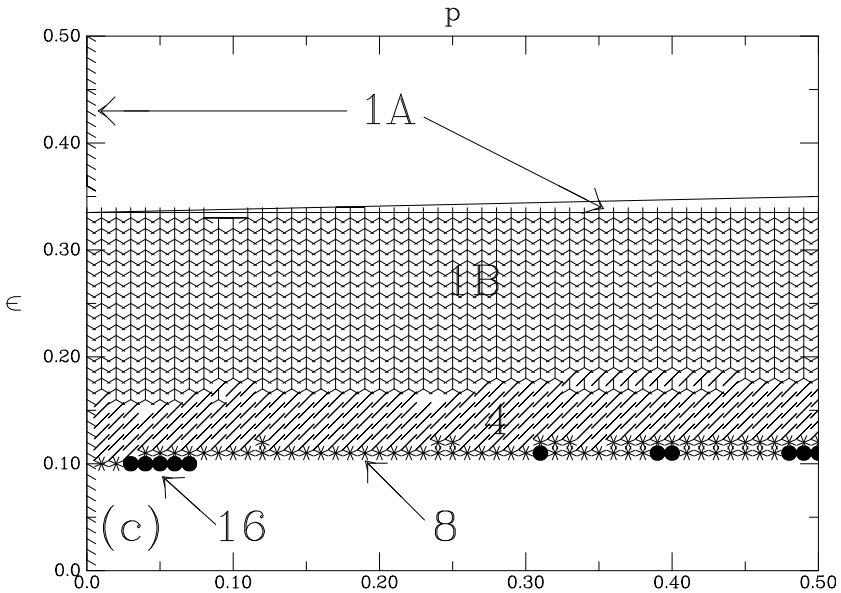
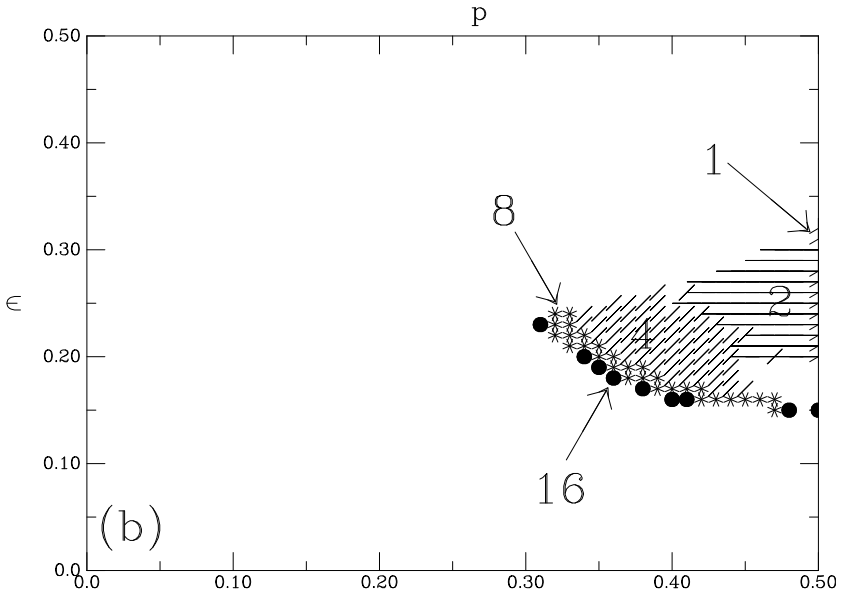
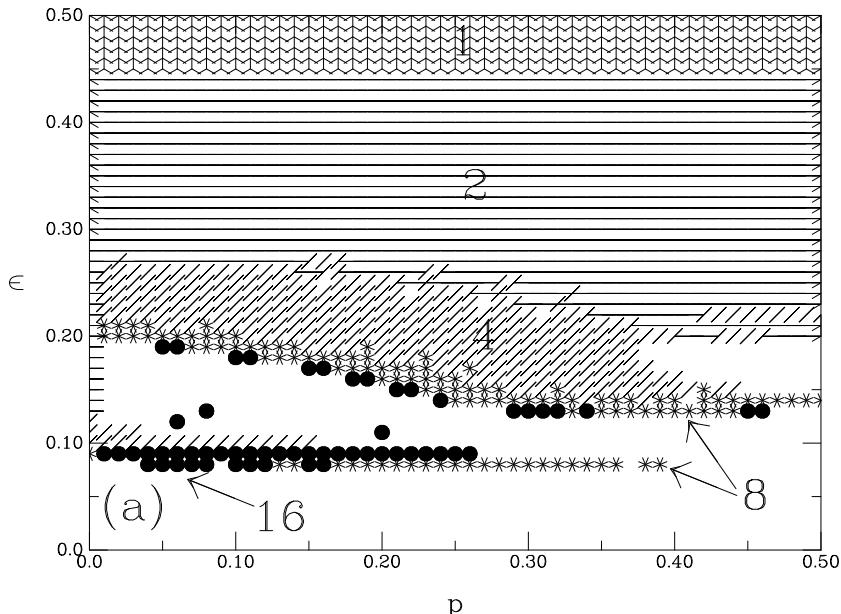


FIG. 3. Regions of periodic motions on the plane (p, ϵ) for different couplings H in GCM systems displaying two clusters. Local parameter is fixed at $r = 1.7$. The numbers on each region indicate the period of H on that region. a) $H = \langle x \rangle$. b) $H = \langle f \rangle$. c) $H = \Delta x$; 1A: there is only one stationary cluster with constant $H = 0$ along the line $p = 0$, bistability occurs on the edge-shaped region: a state of one stationary cluster with $H = 0$ coexist with a state of two out of phase clusters with constant, nonvanishing H ; 1B: there are two out of phase clusters giving constant $H \neq 0$. d) $H = \bar{x}$.

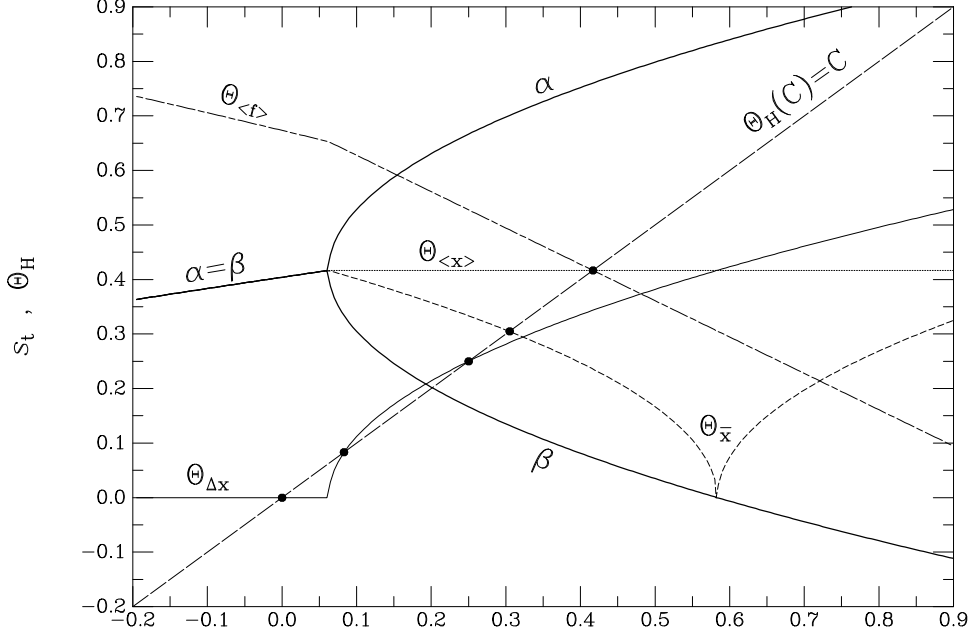


FIG. 4. Bifurcation diagram of the driven map s_t , Eq. (12), with $L_t = C$, as a function of C . The asymptotic orbits of s_t are drawn with solid lines. The values α and β on the period-two window of the driven map are indicated; $\alpha = \beta$ on the fixed point window. The associated coupling functions Θ_H from Eqs. (16)-(19) are also shown vs. C . The intersections with the diagonal $\Theta_H = C$ are indicated by black dots and they correspond to the solutions C_* of Eq. (20)

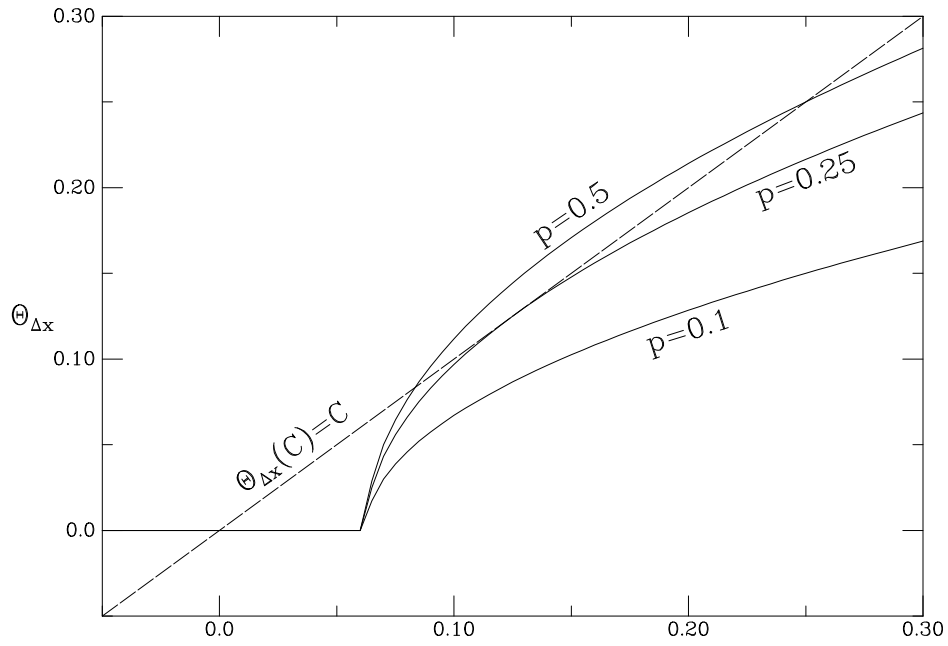


FIG. 5. The associated coupling function $\Theta_{\Delta x}^C$ vs. C for different values of the fraction p . The critical fraction is $p_c = 0.25$. Intersections with the diagonal give the solutions C_* . Solutions for which $\frac{d\Theta}{dC}|_{C_*} > 1$ are unstable.